

See discussions, stats, and author profiles for this publication at: <https://www.researchgate.net/publication/262537375>

Cooperatively Assembling Donor–Acceptor Superstructures Direct Energy Into an Emergent Charge Separated State

ARTICLE *in* JOURNAL OF THE AMERICAN CHEMICAL SOCIETY · MAY 2014

Impact Factor: 12.11 · DOI: 10.1021/ja5015053 · Source: PubMed

CITATIONS

9

READS

57

5 AUTHORS, INCLUDING:



[Karin Adolfsson](#)

KTH Royal Institute of Technology

4 PUBLICATIONS 14 CITATIONS

SEE PROFILE

Cooperatively Assembling Donor–Acceptor Superstructures Direct Energy Into an Emergent Charge Separated State

David Ley, Carmen X. Guzman, Karin H. Adolfsson, Amy M. Scott, and Adam B. Braunschweig*

Department of Chemistry, University of Miami, Coral Gables, Florida 33146, United States

S Supporting Information

ABSTRACT: A novel supramolecular system composed of diketopyrrolopyrrole electron donors and perylene derived bisimide (PDI) electron acceptors forms superstructures that undergo fast photoinduced charge separation following assembly. This bioinspired route toward functional hierarchical structures, whereby assembly and electronic properties are closely coupled, could lead to new materials for artificial photosynthesis and organic electronics.

Natural systems achieve complex optical and electronic properties by employing an “emergence upon assembly” design approach, where new properties that are absent in the individual components arise upon forming hierarchical superstructures composed of pieces with appropriately matched orbital energies.^{1,2} An example of such a system is the photosynthetic reaction center because the precise spatial arrangement of electronically complementary chromophores produces long-distance photoinduced charge separation.³ There is a desire to recreate this bioinspired design strategy for artificial photosynthesis and organic electronics,^{4,5} and a common method to prepare these materials is through covalently linking electron donors, acceptors, and light harvesting antenna systems.^{6–9} But as the building blocks grow larger and more complex, attempts to covalently link all the pieces confront the limits of synthetic chemistry. As an alternative, supramolecular assembly is increasingly employed to build superstructures that undergo photoinduced charge separation.^{6,10–15} In doing so, scientists harness the inherent error correcting nature of noncovalent assembly and achieve structural complexity through significantly shorter syntheses. Chromophore arrays have been successfully prepared using hydrogen bonding (H-bonding),^{16–18} $\pi\cdots\pi$ stacking,¹⁹ and other supramolecular approaches,^{20–23} but how the superstructures affect the optoelectronic properties is still an area of investigation because only in a few of these systems have both assembly and charge generation been fully characterized. Thus, there is a need to develop more artificial photosynthetic systems that simultaneously (1) are composed of synthetically modular components, where frontier molecular orbital (FMO) levels, electronic coupling, and absorption can be systematically tuned, (2) assemble into architecturally complex superstructures, and (3) direct photochemical excitation into a charge separated state.

We have recently described a supramolecular system composed of the electron-rich organic donor diketopyrrolo-

pyrrole (DPP)²⁴ and the electron-poor organic acceptor perylene derived bisimide (PDI) (Figure 1A)²⁵ that forms

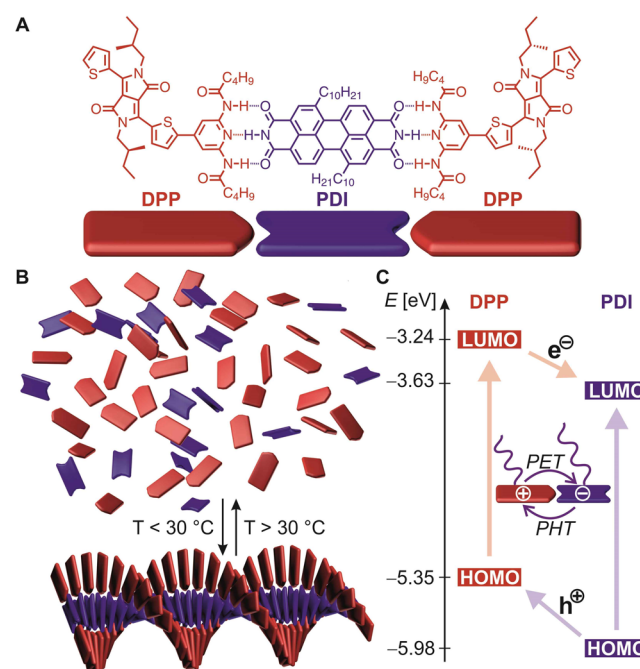


Figure 1. (A) H-bonding brings the DPP donor (red) and the PDI acceptor (blue) together. (B) Upon cooling, superstructures arise from H-bonding and orthogonal π - π stacking. (C) FMO scheme indicating possible photoinduced electron and hole transfer via donor or acceptor excitation.

2:1 coassembled helical supramolecular polymers as a result of triple H-bonding between the PDI and the DPP and π - π stacking orthogonal to the H-bonding axis (Figure 1B).²⁶ Both donor and acceptor are prepared in few synthetic steps, where changing the substituents on the DPPs or PDIs modify the bandgap and absorption maxima. Herein, we report the electronic and optical properties of these assemblies and demonstrate that charge transfer is directed by reversible supramolecular interactions. The two chromophores are electronically complementary in that the FMO levels are positioned such that upon photoexcitation, charge transfer can possibly occur by either hole transfer from PDI to DPP or by electron transfer from the DPP to the PDI (Figure 1C). Results

Received: February 12, 2014

Published: May 20, 2014



of our photophysical studies confirm that indeed photoinduced electron transfer is not possible between the disaggregated individual components alone, but only emerges upon superstructure formation. This donor–acceptor system exemplifies how supramolecular assembly and FMOs can be synergistically designed to achieve emergent charge transfer in hierarchical organic superstructures.

The synthesis and cooperative assembly of the DPP donor and PDI acceptor components, as well as a *N,N'*-dicyclohexyl-substituted PDI that is unable to bind DPP, are described in detail elsewhere.²⁶ The system assembles into helical superstructures via a cooperative equilibrium that can be switched off or on by varying the temperature or concentration. At high temperature or low concentration, disaggregation is favored, while at low temperature and high concentration, entropically disfavored supramolecular polymerization drives the formation of superstructures with a 2:1 donor:acceptor ratio.

Having demonstrated the biomimetic assembly that uses multiple noncovalent interactions operating in concert, we proceeded to assess the capability of the system to undergo photoinduced charge separation and subsequent charge migration with the aim of creating a long-lived radical pair state that is a prerequisite for harvesting the resulting photochemical energy. The ground-state FMO energy levels of the individual DPP and PDI compounds were investigated by cyclic voltammetry (CV), UV–vis, and fluorescence spectroscopy to determine whether the components were properly designed to undergo thermodynamically favored charge separation upon assembly. These studies revealed that electron transfer could proceed from the upper SOMO (−3.24 eV) of photoexcited DPP into the PDI LUMO (−3.63 eV) or by respective hole transfer from the lower SOMO (−5.35 eV) of photoexcited PDI into the DPP HOMO (−5.98 eV) with driving forces of −0.39 and −0.63 eV, respectively.²⁷ Variable temperature (VT) fluorescence spectroscopy was employed to determine if fluorescence quenching, indicative of charge separation, occurs upon temperature-induced aggregation. A 2:1 solution of DPP (45 μM) to PDI (23 μM) in toluene was prepared, and the fluorescence spectra were measured from 500–800 nm at 12 temperatures ranging from 70 to 20 $^{\circ}\text{C}$. The solution was photoexcited at 356 nm (Figure 2A), where the DPP absorbance is three times greater than that of PDI, providing for quasiselective photoexcitation. As controls, individual components as well as a mixture where the PDI was replaced by its *N,N'*-dicyclohexyl-substituted derivative that is unable to aggregate were measured under the same conditions.²⁷

The VT fluorescence shows that aggregation driven static quenching occurs as a likely result of charge separation, which we later confirm using femtosecond transient absorption (fs-TA) spectroscopy. As a thermally disaggregated sample (70 $^{\circ}\text{C}$) is cooled down, the DPP fluorescence intensity initially increases (Figure 2A) because nonradiative decay of an excited state is typically promoted at higher temperatures (dynamic quenching). The fluorescence intensity reaches a maximum at 40 $^{\circ}\text{C}$ before it drops with decreasing temperatures, as a result of static quenching, and finally stabilizes at 20 $^{\circ}\text{C}$. Most importantly, the absorbance of the sample at the excitation wavelength 356 nm does not change with temperature,²⁷ and there is no decrease in DPP fluorescence in the absence of the PDI, which means that aggregation-induced quenching is not occurring. This indicates that fluorescence quenching is an emergent property that arises with the noncovalent assembly of

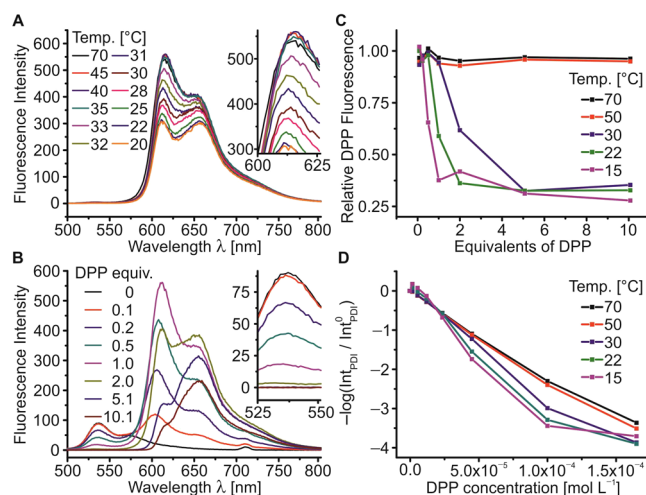


Figure 2. (A) VT fluorescence spectra of a 2:1 DPP:PDI mixture (45 and 23 μM , respectively) in toluene (λ_{Ex} = 356 nm). (B) Fluorescence titration at 30 $^{\circ}\text{C}$ (λ_{Ex} = 356 nm), molar equivalents of DPP given based on PDI. (C) Relative DPP fluorescence intensity at various temperatures. (D) Fluorescence quenching of PDI with increasing DPP concentration at various temperatures.

heterosuperstructures, which begin to form around 30 $^{\circ}\text{C}$.²⁶ Further support for this concept comes from dynamic light scattering measurements,²⁷ showing that the formation of large ($\sim 1\text{--}2\ \mu\text{m}$) superstructures occurs concomitantly with fluorescence quenching.

The effects of temperature and concentration on the aggregation induced quenching were further investigated by a VT fluorescence titration (Figure 2B). To a solution of PDI in toluene (25 μM), a solution of DPP in toluene (481 μM) was added, and the fluorescence spectra were measured at 356 and 483 nm excitation at five temperatures and seven concentrations. The resulting spectra were compared to that of the individual components, so spectral changes that occur because of aggregation could be unambiguously assigned.²⁷ The relative fluorescence intensity of the DPP (Figure 2C) is the ratio of DPP fluorescence in the mixture to that of DPP alone under the same conditions, and this plot depicts the quenching of DPP fluorescence that is induced by temperature and concentration-dependent heteroaggregation. Excess DPP units in the heteroaggregates can act as antennas transferring excitation energy toward the next donor–acceptor pair, thus explaining the observed quenching at DPP:PDI ratios $>2:1$. A similar analysis for the PDI is not possible since the DPP absorbs fluorescence photons of the PDI. This emission–absorption produces a linear plot at temperatures that disfavor aggregation, and the deviation from this linearity occurring at $T < 30\ ^{\circ}\text{C}$ (Figure 2D) indicates that the PDI fluorescence is partly quenched by the DPP because temperature-dependent heteroaggregation brings the donor and acceptor close enough for charge separation. Photoexcited PDI could transfer its energy to the DPP via Förster resonance energy transfer, another viable explanation for fluorescence quenching, but this possibility can be ruled out because the DPP would then exhibit a relative fluorescence intensity greater than unity, which was not observed. Terminal H-bonding is crucial for the superstructure formation,²⁶ and no fluorescence quenching can be observed for the *N,N'*-dicyclohexyl protected PDI, which is incapable of H-bonding or superstructure formation.²⁷

To further investigate the photoinduced charge-transfer process, fs-TA experiments were performed at room temperature on the individual compounds and on the 2:1 DPP:PDI mixture in toluene. Photoexcitation of DPP (83 μM) at 485 nm with ~ 150 fs laser pulses (Figure S45) results in the appearance of ground-state bleaching at (b) 544 and (e) 594 nm. The ground state recovers monoexponentially with time constants around 5 ns (Table S5), which is near the limitation of the detection window. This agrees with fluorescence lifetimes (τ_{FL} , $S_0 \leftarrow S_1$) for comparable structures.²⁸ Positive transient features between 700 and 800 nm (g–i) decay with longer time constants, indicating that the S_1 state undergoes inefficient singlet triplet crossing^{28,29} with a time constant that is approximately two times longer than the fluorescence lifetime, hampering a detailed kinetic analysis in this spectral range. The fs-TA spectrum of the PDI (Figure S46) shows a pronounced ground-state bleaching feature at (a) 523 nm, which is red-shifted compared to the ground-state absorption band at 519 nm because of contributions from stimulated emission. The negative feature at (d) 578 nm arises from stimulated emission alone (Figure S51). The recoveries are dominated by time constants of >6 ns and 4.7 ± 0.1 ns. A broad positive feature (650–785 nm, g) represents the S_1 state of the PDI.³⁰

The fs-TA spectrum of a 2:1 mixture (Figure 3) of DPP (83 μM) and PDI (42 μM) contains a pronounced ground-state

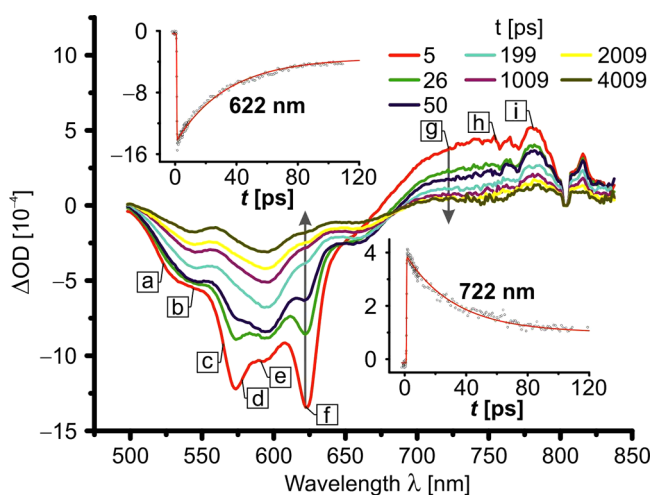


Figure 3. fs-TA spectra of the 2:1 (DPP:PDI) mixture in toluene with absorption vs time profiles of (upper inset) the ground-state absorption band of the supramolecular DPP-PDI aggregate at $\lambda = 622$ nm and (lower inset) the positive feature at $\lambda = 722$ nm. Arrows denote the peaks at 622 and 722 nm. The assignments and lifetimes of each of the labeled peaks (a–i) are provided in Table S5.

bleach at (f) 622 nm, which is not present in the spectra of the individual components and corresponds to the supramolecular aggregate, as we have previously shown.²⁶ This feature displays a fast rise within the 200 fs instrument response time, and the ground state recovers following biexponential kinetics with a fast component of 33.1 ± 0.5 ps (76%) and a slow component of 3.74 ± 0.18 ns (24%). The slow component originates from overlap with the neighboring signals. Concomitant with the recovery of this new ground-state bleach is the decay of the positive feature at 722 nm (31.9 ± 0.7 ps, 71%) from $\text{PDI}^{\bullet-}$ (g). These data are in good agreement with the spectral positions of previously reported, similar PDI-based systems,^{30–32} and are also in excellent agreement with the

absorption maximum of the radical anion of our PDI system,²⁷ which we obtained by chemical reduction with F^- ,²⁷ following the method reported by Saha et al.^{33,34} The broad $\text{PDI}^{\bullet-}$ absorption signal may indicate charge migration through stacked PDIs in the supramolecular aggregate, as it has been previously shown that aggregation-induced migration broadens the absorption of $\text{PDI}^{\bullet-}$ and concomitantly lowers its intensity.¹⁴ Following chemically-induced disaggregation with 5% DMSO, which interrupts H-bonding, the TA dynamics within the 2:1 DPP:PDI mixture resemble a linear combination of the individual compounds. While the recoveries of all ground-state bleaches in the 2:1 mixture show a significant amount of a very fast component (~ 30 ps, see Table S5), upon DMSO-induced disassembly these very fast components vanish, and the intense ground-state bleach at 622 nm disappears entirely.

The absence of fluorescence upon excitation of the aggregate at 622 nm (Figure S9)²⁷ confirms the ultrafast decay via charge recombination. This hypothesis was further supported by calculating the charge separation energy (ΔG_{CS}) in toluene using the Weller equation (eq S4),^{27,35} which estimates ΔG_{CS} to 2.0 eV (620 nm), indicating that the absorption band of the aggregate corresponds to direct photoexcitation into the charge separated state. Calculation of the static reorganization energy λ_s by invoking the Marcus relation (eq S6),^{27,36–39} which is based on the dielectric continuum model of the solvent, yields $\lambda_s = 0.03$ eV. As expected for toluene as a low-polarity solvent, this static contribution is insignificant, so that the overall reorganization energy is given by the intrinsic value λ_i , which we determined by using density functional theory computations employing the ORCA program package.^{27,40} The overall reorganization energy λ was calculated to be 0.33 eV, which is very close to the absolute value of ΔG for charge separation from photoexcited PDI (Figure 4). This charge separation

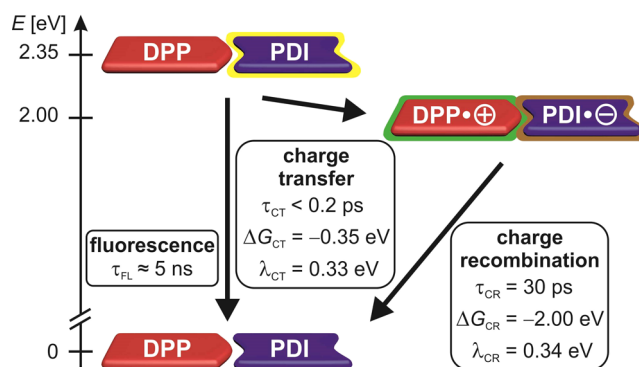


Figure 4. Energy diagram of a DPP-PDI assembly in toluene. Photoexcited DPP (2.07 eV) is not shown, as it is almost isoenergetic with the charge-transfer state (2.0 eV). Band gaps were evaluated using absorption and emission spectroscopy, while the energy of the charge separated state was calculated by performing the Weller correction on the reduction and oxidation potentials.

(τ_{CS}) must therefore occur closely between the normal and the inverted Marcus regime and is very fast. Owing to the much larger free enthalpy of the charge recombination ($\Delta G_{\text{CR}} = -2.0$ eV), the lifetime of this process (τ_{CR}) is 30 ps, indicating that it occurs in the Marcus inverted regime.³⁹ However, τ_{CR} is also sensitive to the electronic coupling^{41,42} which may contribute greatly to the fast τ_{CR} .⁴³

In conclusion, we have used fluorescence and transient absorption spectroscopy to show that photoexcitation of donor–acceptor superstructures with visible light directs the system into a charge separated state. Importantly cooperative noncovalent bonding and FMO levels were synergistically designed to achieve new photophysical properties that emerge only upon assembly. The presence of the charge-transfer band at 622 nm indicates a more subtle electronic interaction between donors and acceptors upon self-assembly, and the nature of this interaction will be further investigated in the future. We intend to build upon this system that combines easily modified components and convergent supramolecular assembly to increase charge separation lifetimes, explore the influence of superstructure shape upon charge migration, and, ultimately, create new systems for solar energy harvesting and molecular electronics.

■ ASSOCIATED CONTENT

■ Supporting Information

Experimental details, spectra, and further data. This material is available free of charge via the Internet at <http://pubs.acs.org>.

■ AUTHOR INFORMATION

Corresponding Author

a.braunschweig@miami.edu

Notes

The authors declare no competing financial interest.

■ ACKNOWLEDGMENTS

A.B.B. is grateful to the Army Research Office (W911NF-12-1-0125 and W911NF-14-1-0164) for generous support. The authors thank F. Raymo and Ultrafast Systems for access to instrumentation and David I. Schuster for guidance.

■ REFERENCES

- (1) Remy, A.; Gerwert, K. *Nat. Struct. Mol. Biol.* **2003**, *10*, 637.
- (2) Lawrence, D. S.; Jiang, T.; Levett, M. *Chem. Rev.* **1995**, *95*, 2229.
- (3) Cogdell, R. J.; Gall, A.; Köhler, J. Q. *Rev. Biophys.* **2006**, *39*, 227.
- (4) Gust, D.; Moore, T. A.; Moore, A. L. *Acc. Chem. Res.* **2000**, *34*, 40.
- (5) Fukuzumi, S. *Phys. Chem. Chem. Phys.* **2008**, *10*, 2283.
- (6) Wasielewski, M. R. *Acc. Chem. Res.* **2009**, *42*, 1910.
- (7) Saha, S.; Stoddart, J. F. *Chem. Soc. Rev.* **2007**, *36*, 77.
- (8) Imahori, H.; Guldi, D. M.; Tamaki, K.; Yoshida, Y.; Luo, C.; Sakata, Y.; Fukuzumi, S. *J. Am. Chem. Soc.* **2001**, *123*, 6617.
- (9) de Miguel, G.; Wielopolski, M.; Schuster, D. I.; Fazio, M. A.; Lee, O. P.; Haley, C. K.; Ortiz, A. L.; Echegoyen, L.; Clark, T.; Guldi, D. M. *J. Am. Chem. Soc.* **2011**, *133*, 13036.
- (10) Würthner, F.; Chen, Z.; Hoeben, F. J. M.; Osswald, P.; You, C.-C.; Jonkhuyzen, P.; Herrikhuizen, J. v.; Schenning, A. P. H. J.; van der Schoot, P. P. A. M.; Meijer, E. W.; Beckers, E. H. A.; Meskers, S. C. J.; Janssen, R. A. J. *J. Am. Chem. Soc.* **2004**, *126*, 10611.
- (11) Wessendorf, F.; Grimm, B.; Guldi, D. M.; Hirsch, A. *J. Am. Chem. Soc.* **2010**, *132*, 10786.
- (12) Frischmann, P. D.; Mahata, K.; Würthner, F. *Chem. Soc. Rev.* **2013**, *42*, 1847.
- (13) Grimm, B.; Schornbaum, J.; Jasch, H.; Trukhina, O.; Wessendorf, F.; Hirsch, A.; Torres, T.; Guldi, D. M. *Proc. Natl. Acad. Sci. U.S.A.* **2012**, *109*, 15565.
- (14) van der Boom, T.; Hayes, R. T.; Zhao, Y.; Bushard, P. J.; Weiss, E. A.; Wasielewski, M. R. *J. Am. Chem. Soc.* **2002**, *124*, 9582.
- (15) Wasielewski, M. R. *J. Org. Chem.* **2006**, *71*, 5051.
- (16) Bushey, M. L.; Nguyen, T.-Q.; Zhang, W.; Horoszewski, D.; Nuckolls, C. *Angew. Chem., Int. Ed.* **2004**, *43*, 5446.
- (17) Jimenez, A. J.; Calderon, R. M. K.; Rodriguez-Morgade, M. S.; Guldi, D. M.; Torres, T. *Chem. Sci.* **2013**, *4*, 1064.
- (18) Wang, F.; Gillissen, M. A. J.; Stals, P. J. M.; Palmans, A. R. A.; Meijer, E. W. *Chem.—Eur. J.* **2012**, *18*, 11761.
- (19) Gunderson, V. L.; Smeigh, A. L.; Kim, C. H.; Co, D. T.; Wasielewski, M. R. *J. Am. Chem. Soc.* **2012**, *134*, 4363.
- (20) Würthner, F.; Kaiser, T. E.; Saha-Möller, C. R. *Angew. Chem., Int. Ed.* **2011**, *50*, 3376.
- (21) Cañas-Ventura, M. E.; Ait-Mansour, K.; Ruffieux, P.; Rieger, R.; Müllen, K.; Brune, H.; Fasel, R. *ACS Nano* **2010**, *5*, 457.
- (22) Safont-Sempere, M. M.; Fernández, G.; Würthner, F. *Chem. Rev.* **2011**, *111*, 5784.
- (23) Shahar, C.; Baram, J.; Tidhar, Y.; Weissman, H.; Cohen, S. R.; Pinkas, I.; Rybtchinski, B. *ACS Nano* **2013**, *7*, 3547.
- (24) Tamayo, A. B.; Tantiwivat, M.; Walker, B.; Nguyen, T.-Q. *J. Phys. Chem. C* **2008**, *112*, 15543.
- (25) Würthner, F. *Chem. Commun.* **2004**, 1564.
- (26) Rieth, S.; Li, Z.; Hinkle, C. E.; Guzman, C. X.; Lee, J. J.; Nehme, S. I.; Braunschweig, A. B. *J. Phys. Chem. C* **2013**, *117*, 11347.
- (27) Further details in the Supporting Information.
- (28) Karsten, B. P.; Bouwer, R. K. M.; Hummelen, J. C.; Williams, R. M.; Janssen, R. A. J. *Photochem. Photobiol. Sci.* **2010**, *9*, 1055.
- (29) Karsten, B. P.; Smith, P. P.; Tamayo, A. B.; Janssen, R. A. J. *J. Phys. Chem. A* **2012**, *116*, 1146.
- (30) Gosztola, D.; Niemczyk, M. P.; Svec, W.; Lukas, A. S.; Wasielewski, M. R. *J. Phys. Chem. A* **2000**, *104*, 6545.
- (31) Jiménez, A. J.; Grimm, B.; Gunderson, V. L.; Vagnini, M. T.; Krick Calderon, S.; Rodríguez-Morgade, M. S.; Wasielewski, M. R.; Guldi, D. M.; Torres, T. *Chem.—Eur. J.* **2011**, *17*, 5024.
- (32) Rodríguez-Morgade, M. S.; Torres, T.; Atienza-Castellanos, C.; Guldi, D. M. *J. Am. Chem. Soc.* **2006**, *128*, 15145.
- (33) Guha, S.; Goodson, F. S.; Corson, L. J.; Saha, S. *J. Am. Chem. Soc.* **2012**, *134*, 13679.
- (34) Goodson, F. S.; Panda, D. K.; Ray, S.; Mitra, A.; Guha, S.; Saha, S. *Org. Biomol. Chem.* **2013**, *11*, 4797.
- (35) Weller, A. Z. *Phys. Chem.* **1982**, *133*, 93.
- (36) Marcus, R. A. *J. Chem. Phys.* **1956**, *24*, 966.
- (37) Greenfield, S. R.; Svec, W. A.; Gosztola, D.; Wasielewski, M. R. *J. Am. Chem. Soc.* **1996**, *118*, 6767.
- (38) Scott, A. M.; Miura, T.; Ricks, A. B.; Dance, Z. E. X.; Giacobbe, E. M.; Colvin, M. T.; Wasielewski, M. R. *J. Am. Chem. Soc.* **2009**, *131*, 17655.
- (39) Barbara, P. F.; Meyer, T. J.; Ratner, M. A. *J. Phys. Chem.* **1996**, *100*, 13148.
- (40) Neese, F. *WIREs Comput. Mol. Sci.* **2012**, *2*, 73.
- (41) Closs, G. L.; Miller, J. R. *Science* **1988**, *240*, 440.
- (42) Paulson, B. P.; Miller, J. R.; Gan, W.-X.; Closs, G. J. *Am. Chem. Soc.* **2005**, *127*, 4860.
- (43) Jakob, M.; Berg, A.; Stavitski, E.; Chernick, E. T.; Weiss, E. A.; Wasielewski, M. R.; Levanon, H. *Chem. Phys.* **2006**, *324*, 63.